

Enhancing Non-classical Properties of Entangled Coherent States via Post-Selected von Neumann Measurements

Janarbek Yuanbek^{1,2*} and Bruno Tenorio³

¹*State Key Laboratory of Semiconductor Physics and Chip Technologies, Institute of Semiconductors, Chinese Academy of Sciences, Beijing 100083, China*

²*Center of Materials Science and Opto-Electronic Technology, University of Chinese Academy of Sciences, Beijing 100049, China and*

³*Wolfram Research South America, Lima 15076, Peru*

(Dated: December 2, 2025)

The present study systematically investigates the modulation mechanism of post-selected weak measurement (WM) on the non-classical properties of entangled coherent states (ECSs). The primary goal is achieving controllable enhancement of quantum resources such as entanglement and squeezing, while minimising disturbance to the quantum state. We theoretically analyse the post-selected weak measurement process, and its effectiveness in amplifying the non-classical features of ECSs. The von Neumann measurement model is employed to analytically describe the weak-value amplification of the pointer state. It is demonstrated that a significant enhancement of squeezing can be achieved by tuning the measurement coupling strength. The joint Wigner function analysis in phase space further reveals that, as the coupling strength increases, the coherent structure of the state evolves from symmetric double peaks to multi-branch quantum interference fringes. The entanglement, quantified by the Hillery-Zubairy criterion, exhibits a pronounced increase with stronger coupling, while the quantum Fisher information indicates a systematic improvement in phase estimation precision. The results obtained establish a tunable weak measurement framework for precise manipulation of continuous-variable entangled states. This provides a feasible theoretical pathway for enhancing quantum metrology and measurement-based state engineering.

I. INTRODUCTION

Weak measurement (WM) initially proposed by Aharonov, Albert, and Vaidman (AAV) in the 1980s, constitutes a conceptual breakthrough that extended quantum measurement beyond the traditional projective (von Neumann) paradigm, thereby profoundly reshaping its theoretical foundations [1]. WM explore the subtle interplay between quantum systems and measuring devices under minimal disturbance. They enable the extraction of weak values (WV) that reveal otherwise inaccessible information about quantum states [2, 3]. Unlike strong measurements that collapse the system into eigenstates, WM preserve quantum coherence. They allow anomalous weak-value amplification (WVA) of specific observables through post-selection or controlled weak interactions, offering a powerful tool for probing non-classical phenomena. Its applicability for quantum state optimization has been explored in various scenarios [4–9], as well its relevance in fundamental aspects of quantum mechanics [10–15]. A critical challenge in this domain lies in understanding how post-selected WM influence the intrinsic properties of entangled quantum states, particularly entangled coherent states (ECSs) [16–18]. ECSs, formed by entangling two coherent states, represent a class of continuous-variable states that bridge discrete quantum logic and continuous-wave optics. They exhibit unique non-classical features such as quadrature squeezing, Einstein-Podolsky-Rosen (EPR) correlations, and sub-Poissonian photon statistics; making them indispensable for quantum communication, metrology, and computation [19–21]. However,

their sensitivity to measurement-induced disturbances has remained an open question. While conventional strong measurements often degrade entanglement and non-classicality, the role of WMs, especially those leveraging post-selection, remains less explored [22].

Prior research has demonstrated that WM can enhance quantum correlations in single-mode systems, such as amplifying weak signals or revealing anomalous WV [23]. Yet, the extension to two-mode ECSs introduces additional complexities: the interplay between mode entanglement, quadrature squeezing, and post-selection effects demands a nuanced analysis. Recent studies on continuous-variable systems have hinted at the potential of WM to reshape quantum statistics and entanglement [24–26]. However, a systematic investigation into how post-selected von Neumann interactions modify the fundamental properties of ECSs such as squeezing, photon statistics and EPR correlations has yet to be fully realized. This gap motivates our study, which builds upon the WM framework to elucidate how post-selection transforms ECSs, offering insights for quantum state engineering and measurement-based quantum technologies.

In this paper, we investigate how post-selected weak measurements influence the dynamics of ECSs within the framework of the von Neumann measurement model, analyzing the evolution of quantum states under measurement interactions. Setting $\hbar = 1$, we systematically examine the influence of measurement parameters on quantum compression, phase distribution, and entanglement properties. Our results show that tuning the coupling strength effectively enhances non-classical characteristics, with a significant improvement in entanglement. Furthermore, we demonstrate via quantum Fisher information that the scheme enhances parameter estimation precision.

* janarbek@semi.ac.cn

The remainder of this paper is organized as follows. Section II outlines the theoretical framework for post-selected weak measurements. Section III analyzes the effects on sum squeezing. Section IV examines the joint Wigner function in phase space. Section V investigates entanglement properties using the Hillery-Zubairy criterion. Section VI assesses parameter estimation precision through quantum Fisher information. The paper concludes with a summary of implications in Section VII.

II. THEORETICAL FRAMEWORK

We begin by considering an ECSs [16, 27, 28], represented as

$$\begin{aligned} |\phi_i\rangle &= e^{-|\alpha|^2/2} \mathcal{N} \sum_{n=0}^{\infty} \frac{\alpha^n}{n!} [(a_a^\dagger)^n + (a_b^\dagger)^n] |0\rangle_a |0\rangle_b \\ &= \mathcal{N} (|\alpha\rangle_a |0\rangle_b + |0\rangle_a |\alpha\rangle_b), \end{aligned} \quad (1)$$

where $|0\rangle$ and $|\alpha\rangle$ denote the vacuum and coherent states in spatial modes a and b , respectively, and $\mathcal{N} = [2(1 + e^{-|\alpha|^2})]^{-1/2}$ [29], here $\alpha = re^{i\mu}$. A phase shift ϕ is applied to the second mode, described by the unitary operator $\hat{U}(\phi) = \mathbb{I} \otimes e^{i\phi \hat{n}_b}$, where $\hat{n}_b = \hat{b}^\dagger \hat{b}$ is the number operator for mode b . The action of this operator on a coherent state is $e^{i\phi \hat{n}_b} |\alpha\rangle_b = |\alpha e^{i\phi}\rangle_b$. The output state after phase evolution is:

$$|\phi\rangle = \hat{U}(\phi) |\phi_i\rangle = \mathcal{N} (|\alpha\rangle_a |0\rangle_b + |0\rangle_a |\alpha e^{i\phi}\rangle_b). \quad (2)$$

In measurement theory, the total Hamiltonian is generally decomposed into three fundamental components, each governing distinct physical processes during the measurement interaction. These three components are formally expressed as

$$\hat{H} = \hat{H}_s + \hat{H}_p + \hat{H}_{int}, \quad (3)$$

Here, \hat{H}_s denotes the Hamiltonian of the measured system, \hat{H}_p denotes the Hamiltonian of the measuring apparatus (pointer), and \hat{H}_{int} characterizes the interaction between the system and the apparatus. Within the framework of ideal measurement theory [30], the specific forms of the Hamiltonians describing the pointer and the measured system do not influence the measurement outcomes. Although the pointer and system Hamiltonians are not relevant in defining measurement outcomes, the interaction Hamiltonian plays a crucial role in defining the measurement strength and post-selection effects. In this study, we adopt the interaction Hamiltonian as [31]

$$\hat{H}_{int} = g_a(t) \hat{\sigma}_x \otimes \hat{P}_x + g_b(t) \hat{\sigma}_y \otimes \hat{P}_y, \quad (4)$$

where $g(t)$ describes the time-dependent coupling strength between the measured system and pointer, such that is non-zero on finite intervals, and its time-integrated value is represented as $\int_{t_0}^t g(\tau) d\tau = g\delta(t - t_0)$, $\hat{\sigma}_x$ is the measured observable, and (\hat{P}_x, \hat{P}_y) are the pointer momentum operators

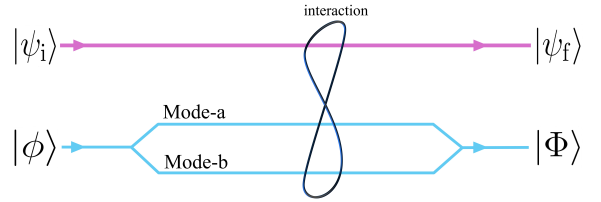


Figure 1. Schematic diagram of weak measurement theory and setup for preparing the state $|\Phi\rangle$ using a post-selected von Neumann measurement. Schematic diagram of the measurement on mode-a, showing three key steps: (1) Preparation: The measured system and pointer are initially prepared in states $|\psi_i\rangle$ and $|\phi\rangle$, respectively. (2) Weak Interaction: A weak interaction between the measured system and measuring device governs the evolution of the composite system. (3) Post-selection: Following evolution, the composite system is projected onto the measured system state $|\Phi\rangle$, deliberately and technically chosen to obtain the desired system observable values.

which are conjugate to the pointer position operators (\hat{X}, \hat{Y}) satisfying $[\hat{X}, \hat{P}_x] = [\hat{Y}, \hat{P}_y] = i$. Both operators can be expressed via annihilation ($\hat{a}^\dagger, \hat{b}^\dagger$) and creation (\hat{a}, \hat{b}) operators as $\hat{P}_x = i(\hat{a}^\dagger - \hat{a})/2\sigma$ and $\hat{P}_y = i(\hat{b}^\dagger - \hat{b})/2\sigma$ [32], where $\sigma = \sqrt{1/2m\omega}$ represents the Gaussian ground-state width of the pointer, determined by its mass m and oscillation frequency ω . In Fig. 1 we illustrate the experimental setup of weak interactions. Based on this, the initial composite state is given by:

$$|\Psi_{in}\rangle = |\psi_i\rangle \otimes |\phi\rangle, \quad (5)$$

where

$$|\psi_i\rangle = \cos \frac{\theta}{2} |H\rangle + e^{i\delta} \sin \frac{\theta}{2} |V\rangle, \quad (6)$$

here, $\delta \in [0, 2\pi]$, $\theta \in [0, \pi)$ and $|\phi\rangle$ are the initial states of the measured system and pointer. In a post-selected von Neumann measurement, the system is defined by both pre- and post-selection of its state. We prepare the system in an initial state $|\psi_i\rangle$ and then we couple it to the pointer state. After some interaction time t_0 , we post-select a system state $|\psi_f\rangle$, and obtain information on the physical quantities $\hat{\sigma}_x$ and $\hat{\sigma}_y$ from the pointer wave function. If we set the post-selection to $|\psi_f\rangle = |\uparrow_z\rangle$, we obtain the following weak values

$$\langle \hat{\sigma}_x \rangle_w = \frac{\langle \psi_f | \hat{\sigma}_x | \psi_i \rangle}{\langle \psi_f | \psi_i \rangle} = e^{i\delta_1} \tan \frac{\theta_1}{2}. \quad (7)$$

$$\langle \hat{\sigma}_y \rangle_w = \frac{\langle \psi_f | \hat{\sigma}_y | \psi_i \rangle}{\langle \psi_f | \psi_i \rangle} = -ie^{i\delta_2} \tan \frac{\theta_2}{2}. \quad (8)$$

Where $\delta = [0, 2\pi]$ and $\theta = [0, \pi)$. In general, the weak value is a complex quantity. It is evident from Eqs.7 and 8 that when the pre-selected state $|\psi_i\rangle$ and the post-selected state $|\psi_f\rangle$ are nearly orthogonal, the absolute value of the weak

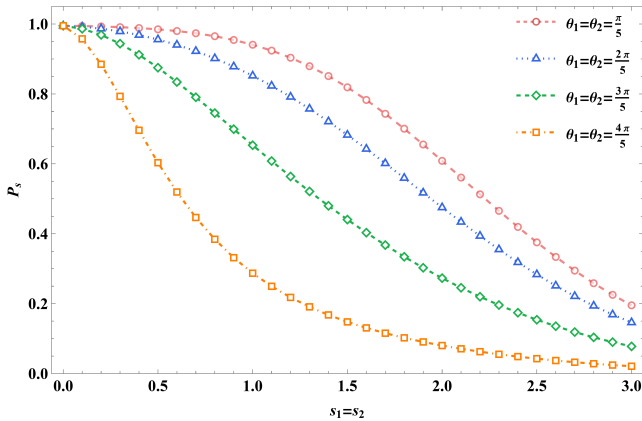


Figure 2. Post-selection success probability of the final pointer state $|\Phi\rangle$ as a function of coupling strength ($s_1 = s_2$) for different weak value parameters ($\theta_1 = \theta_2$), with the parameters $\mu = \varphi = \delta_1 = \delta_2 = \pi/2$, and $r = 0.1$.

value can be arbitrarily large, resulting in the weak-value amplification. From the above definitions, we have the unitary evolution operators $e^{-ig_a\hat{\sigma}_x\otimes\hat{P}_x}$ and $e^{-ig_b\hat{\sigma}_y\otimes\hat{P}_y}$, such that the operator \hat{A} in the system space that satisfies the property $\hat{A}^2 = \hat{I}$, then the evolution operators can be expressed as follows:

$$e^{-ig_a\hat{\sigma}_x\otimes\hat{P}_x} = \frac{1}{2} \left[(\hat{I} + \hat{\sigma}_x) \otimes D\left[t\frac{g_a}{2\sigma}\right] + (\hat{I} - \hat{\sigma}_x) \otimes D^\dagger\left[t\frac{g_a}{2\sigma}\right] \right],$$

$$e^{-ig_b\hat{\sigma}_y\otimes\hat{P}_y} = \frac{1}{2} \left[(\hat{I} + \hat{\sigma}_y) \otimes D\left[t\frac{g_b}{2\sigma}\right] + (\hat{I} - \hat{\sigma}_y) \otimes D^\dagger\left[t\frac{g_b}{2\sigma}\right] \right].$$

We define the displacement operator as $D[s_i/2] = \exp[a^\dagger s_i/2 - a(s_i/2)^*]$, where $s_i = tg_{a,b}/\sigma$ for $i = 1, 2$ is coupling strength parameter. Given that s_i is real ($s_i \in \mathbb{R}$), we set $s_1 = g_1/2\sigma$ and $s_2 = g_2/2\sigma$, which simplifies the expressions to $D[s_1] = \exp[s_1(a^\dagger - a)]$ and $D[s_2] = \exp[s_2(b^\dagger - b)]$. The initial total state is $|\Psi\rangle = |\psi_i\rangle \otimes |\phi\rangle$, after interaction the initial state becomes as

$$|\Psi\rangle = e^{-ig\hat{\sigma}_x\otimes\hat{P}_x} e^{-ig\hat{\sigma}_y\otimes\hat{P}_y} |\psi_i\rangle \otimes |\phi\rangle$$

$$= \frac{1}{4} \left[t_+ D\left[\frac{s_1 + s_2}{2}\right] + t_- D^\dagger\left[\frac{s_1 + s_2}{2}\right] \right. \\ \left. + t'_+ D^\dagger\left[\frac{s_1 - s_2}{2}\right] + t'_- D\left[\frac{s_1 - s_2}{2}\right] \right] |\psi_i\rangle \otimes |\phi\rangle, \quad (9)$$

where $t_\pm = (\hat{I} \pm \hat{\sigma}_x)(\hat{I} \pm \hat{\sigma}_y)$, and $t'_\pm = (\hat{I} \mp \hat{\sigma}_x)(\hat{I} \pm \hat{\sigma}_y)$. In a post-selected von Neumann measurement, the state $|\Psi\rangle$ is projected onto the post-selected state $|\psi_f\rangle$ yields a not normalized pointer state $|\tilde{\Phi}\rangle = \langle\psi_f|\Psi\rangle$. The final normalized probe state is

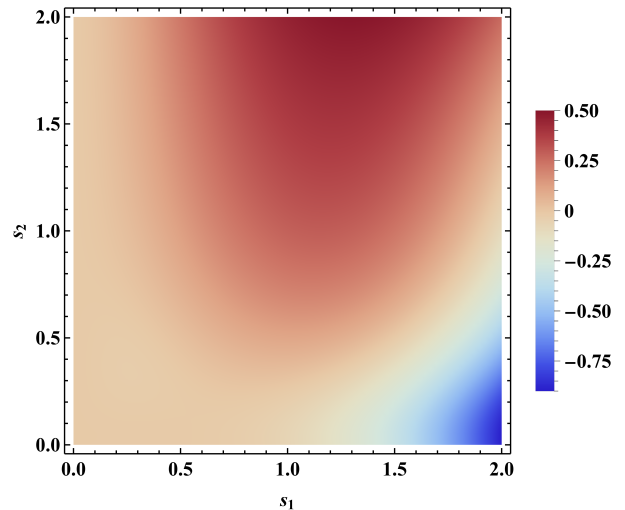


Figure 3. The variation of sum squeezing (S_{2s}) in the state $|\Phi\rangle$ as a function of coupling coefficients s_1 and s_2 , with the parameters $\Theta = \mu = \varphi = \delta_1 = \delta_2 = \pi/2$, $\theta_1 = \theta_2 = 4\pi/5$, and $r = 0.1$.

$$|\Phi\rangle = \frac{|\tilde{\Phi}\rangle}{\sqrt{P_s}} = \frac{\kappa}{4} \left\{ A_+ D\left[\frac{s_1 + s_2}{2}\right] + A_- D^\dagger\left[\frac{s_1 + s_2}{2}\right] \right. \\ \left. + B_+ D^\dagger\left[\frac{s_1 - s_2}{2}\right] + B_- D\left[\frac{s_1 - s_2}{2}\right] \right\} \otimes |\phi\rangle, \quad (10)$$

where $\kappa = 1/\sqrt{P_s}$ is the normalization factor and $P_s = \langle\tilde{\Phi}|\tilde{\Phi}\rangle$ denotes the post-selection success probability, $A_\pm = (\hat{I} \pm \langle\hat{\sigma}_x\rangle_w)(\hat{I} \pm \langle\hat{\sigma}_y\rangle_w)$ and $B_\pm = (\hat{I} \mp \langle\hat{\sigma}_x\rangle_w)(\hat{I} \pm \langle\hat{\sigma}_y\rangle_w)$. It is evident that the final pointer state ($|\Phi\rangle$) is contingent upon both the WV and the coupling strength parameters, as shown in Fig. (2). The successful detection probability of this state, denoted as (P_s), decreases as the WV increases in the weak measurement mechanism. However, the selection of larger values for the coupling coefficients s_1 and s_2 has been demonstrated to yield a high success probability, even in the presence of anomalous WV values, which typically yield low probabilities.

In post-selected weak measurements, the value of the observable is expressed as a complex weak value. Its real (Re) and imaginary (Im) components are obtained from the position and momentum shifts of the measurement device, where Fourier transform converts between position and momentum spaces. We then explore how post-selected von Neumann measurements and observable weak values affect the following intrinsic ECSs properties; sum squeezing, joint Wigner functions, Hillery-Zubairy correlations, and quantum Fisher information.

III. EFFECTS ON SUM SQUEEZING

The multi-mode non-classical phenomenon known as sum squeezing [33], for two modes a and b, is characterized by

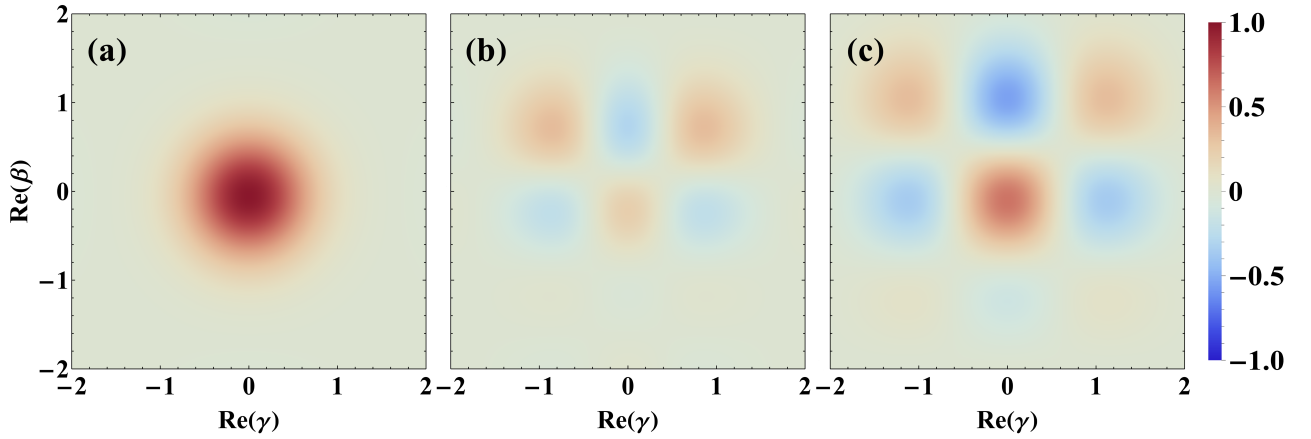


Figure 4. Cross-section of the scaled joint Wigner function $P_J(\gamma, \beta)$ for state $|\Psi\rangle$ in the $\text{Re}(\gamma)$ - $\text{Re}(\beta)$ plane, with $\text{Im}(\gamma) = \text{Im}(\beta) = 0$. (a) $s_1 = s_2 = 0$; (b) $s_1 = s_2 = 1$; (c) $s_1 = s_2 = 2$. Darker shades indicate negative values, a signature of nonclassicality. Other parameters: $r = 0.1$, $\mu = \varphi = \delta_1 = \delta_2 = \pi/2$, and $\theta_1 = \theta_2 = 4\pi/5$.

reduced fluctuations in a particular two-mode quadrature V_Θ observable

$$V_\Theta = \frac{1}{2}(e^{i\Theta}\hat{a}^\dagger\hat{b}^\dagger + e^{-i\Theta}\hat{a}\hat{b}), \quad (11)$$

where Θ is an angle made by V_Θ with the real axis in the complex plane [33–36]. A state is said to be sum squeezed for a value of Θ if $\langle V_\Theta^2 \rangle - \langle V_\Theta \rangle^2 < \langle N_a + N_b + 1 \rangle / 4$, where $N_a = \hat{a}^\dagger\hat{a}$ and $N_b = \hat{b}^\dagger\hat{b}$, then we can define the degree of sum squeezing S_{2s} in the following manner

$$S_{2s} = \frac{4(\langle V_\Theta^2 \rangle - \langle V_\Theta \rangle^2)}{\langle N_a + N_b + 1 \rangle} - 1. \quad (12)$$

The sum squeezing occurs if $S_{2s} < 0$ and a lower bound of S_{2s} is equal to -1 . Hence, the closer the value of S_{2s} to -1 the higher the degree of sum squeezing. By substituting V_Θ in Eq.11 into Eq.12, we obtain S_{2s} in the form of the normal ordered operators

$$S_{2s} = \frac{2 \left[\text{Re}[e^{-2i\Theta}\langle \hat{a}^2\hat{b}^2 \rangle] - 2 \left(\text{Re}[e^{-i\Theta}\langle \hat{a}\hat{b} \rangle] \right)^2 + \langle N_a N_b \rangle \right]}{\langle N_a \rangle + \langle N_b \rangle + 1}. \quad (13)$$

Here, $\langle \dots \rangle$ represents quantum expectation values. Setting $s = 0$ recovers the ECS state $|\phi\rangle$ inherent sum squeezing $S_{2s} = 0$. As demonstrated in Figure 3, the total compression parameter undergoes a continuous evolution from negative to positive values, with the corresponding coupling coefficients s_1 and s_2 varying accordingly. Within the regime of weakly coupled systems, the system primarily exhibits behaviour that is anti-compressive. As coupling coefficients s_1 and s_2 increase, the system undergoes a gradual transition into an enhanced compression state. It is noteworthy that when s_2 is constrained within the weaker region, the magnitude of

s_1 is found to exhibit a substantial amplification in its quantum properties. This result demonstrates that quantum compression behaviour can be effectively manipulated by regulating the coupling strength, enabling flexible switching between compressed and anti-compressed states. This property is of considerable significance for the preparation of non-classical light fields and parameter optimisation in the domain of quantum information processing. In order to provide a robust substantiation for the aforementioned conclusions, the ensuing discourse employs the joint Wigner function as a fundamental tool for validation.

IV. WIGNER FUNCTION

To gain a deeper understanding of the effects of post-selected von Neumann measurements on the properties of the state $|\Psi\rangle$, we examine its phase-space distribution. For our two-mode state $|\Psi\rangle$, the joint Wigner function is defined as:

$$\begin{aligned} W_J(\gamma, \beta) &= \frac{4}{\pi^2} \text{Tr} \left[\rho D(\gamma) D(\beta) P_J D^\dagger(\beta) D^\dagger(\gamma) \right] \\ &= \frac{4}{\pi^2} P_J(\gamma, \beta), \end{aligned} \quad (14)$$

where $\rho = |\Psi\rangle\langle\Psi|$ is the density operator of state $|\Psi\rangle$, and $P_J = P_a P_b = \exp[i\pi a^\dagger a] \exp[i\pi b^\dagger b]$ is the joint photon number parity operator. The operators $D(\gamma) = \exp[\gamma a^\dagger - \gamma^* a]$ and $D(\beta) = \exp[\beta b^\dagger - \beta^* b]$ are the displacement operators acting on the a and b -modes of the two dimensional state $|\Psi\rangle$, respectively. The joint Wigner function W_J describes the state in a four-dimensional (4D) phase space with coordinates $(\text{Re}(\gamma), \text{Im}(\gamma), \text{Re}(\beta), \text{Im}(\beta))$. For our analysis of the phase space distribution of the measurement output state $|\Psi\rangle$, we use the scaled Wigner function $P_J(\gamma, \beta)$ that is bounded within the range of ± 1

$$-1 \leq P_J(\gamma, \beta) \leq 1. \quad (15)$$

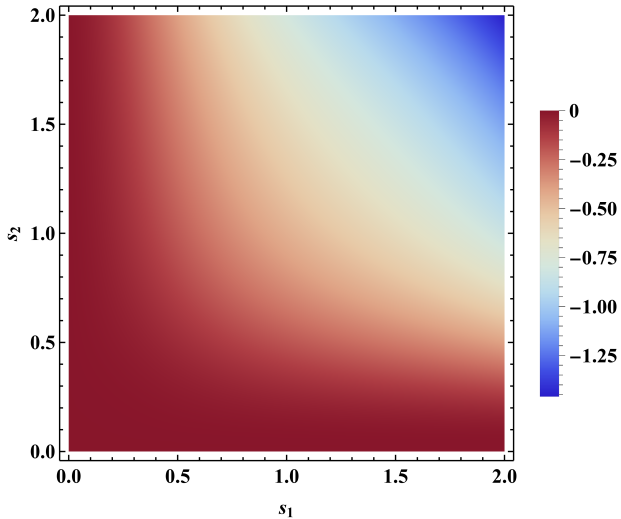


Figure 5. The variation of Hillery-Zubairy correlation(E) in the state $|\Phi\rangle$ as a function of coupling coefficients s_1 and s_2 , with the parameters $\mu = \varphi = \delta_1 = \delta_2 = \pi/2$, $\theta_1 = \theta_2 = 4\pi/5$, and $r = 0.1$.

To highlight the key characteristics of the 4D Wigner function for the state $|\Psi\rangle$ and to compare it with the initial state $|\Psi_i\rangle$, we begin by presenting 2D cross-sections along the $\text{Re}(\gamma)$ and $\text{Re}(\beta)$ plane of the joint Wigner function. From the figure 4, it can be observed that the joint Wigner function $P_j(\gamma, \beta)$ exhibits significant structural evolution with variations in the coupling strength (s_1 and s_2). When $s_1 = s_2 = 0$, the distribution assumes a concentrated symmetric form with a limited range of negative values, indicating weaker non-classical properties in the system. As the parameters increase to $s_1 = s_2 = 1$, the joint distribution develops a multi-branch structure with a markedly enhanced negative region, indicating a pronounced quantum interference effect. Under strong coupling conditions ($s_1 = s_2 = 2$), the negative region further expands to form intricate interference fringes, reflecting the system's highly non-classical behaviour and multi-mode quantum correlations. Overall, this visualisation clearly demonstrates that modulating the coupling strength effectively enhances the system's non-classical properties and entanglement characteristics. Having established these results, we analyze their entanglement structure via the Hillery-Zubairy criterion and study how a post-selected von Neumann measurement affects the quantum correlations in ECSs.

V. HILLERY-ZUBAIRY CORRELATION

The Hillery-Zubairy correlation (HZC) quantifies entanglement in two-mode quantum fields by comparing inter-mode correlations to single-mode photon number expectations [21]. The HZC has important physical implications [37], one way to express the criterion is to define the following quantity:

$$E = \langle \hat{a}^\dagger \hat{a} \rangle \langle \hat{b}^\dagger \hat{b} \rangle - |\langle \hat{a} \hat{b} \rangle|^2. \quad (16)$$

This entanglement criterion underscores the significance of the correlation $\langle \hat{a} \hat{b} \rangle$ between the two modes of a state. Entanglement between the two modes arises when $E < 0$. Additionally, the relation $|\langle \hat{a} \hat{b} \rangle|^2 \leq \langle \hat{a}^\dagger \hat{a} \rangle \langle \hat{b}^\dagger \hat{b} \rangle$ [38] holds, yielding the bound that the entanglement condition for two-mode fields is restricted to $-\langle \hat{a}^\dagger \hat{a} \rangle \leq E < 0$. For the initial pointer state $|\phi\rangle$ the HZC criterion gives $E_\phi = 0.25|\alpha|^2(1 + \exp[-|\alpha|^2])^{-2}$. This result indicates that the EC state $|\phi\rangle$ is a higher-order entangled state as long as $\lambda > 0$. Thus, this condition can always detect entanglement in the state $|\phi\rangle$. We analyze compliance with the HZC criterion for the output state $|\Psi\rangle$ by computing Eq. (16). As illustrated in Fig. (5), the weak value amplification effect demonstrates a substantial enhancement in the entanglement properties within the ECSs. The most significant discovery is the Hillery-Zubairy correlation E , which reveals the amplification of entanglement across a wide spectrum of increasing coupling parameters. This entanglement behaviour indicates the system's precise regulation of entanglement levels, thereby enabling dynamic manipulation of entanglement through external parameters. Consequently, these results emphasise the practical controllability of this system for entanglement manipulation.

VI. CRAMER-RAO BOUND

The potential of post-selection weak measurements for quantum-enhanced metrology thus hinges on a fundamental question: their ability to enhance parameter estimation. To investigate this, we employ the Quantum Fisher Information (QFI) as our core tool. The QFI, computed for a family of initial states, quantifies the maximum information that can be extracted about an unknown parameter. In the case of a pure quantum state, it is defined as

$$Q_{fi} = 4[\langle \Phi' | \Phi' \rangle - |\langle \Phi' | \Phi \rangle|^2], \quad (17)$$

with

$$|\Phi'\rangle = \partial|\Phi\rangle/\partial\varphi = \mathcal{N} \chi \alpha e^{i\varphi} \hat{b}^\dagger |0\rangle_a |\alpha e^{i\varphi}\rangle_b, \quad (18)$$

where $\chi = \kappa\{A \times D[(s_1 + s_2)/2] + B \times D^+[(s_1 - s_2)/2] + C \times D[(s_1 - s_2)/2] + D \times D^+[(s_1 + s_2)/2]\}/4$. The uncertainty in estimating the parameter φ is lower-bounded by the Quantum Cramér-Rao bound (QCRB):

$$\delta\varphi \geq \frac{1}{\sqrt{N Q_{fi}}}, \quad (19)$$

Here, N represents the total number of independent measurements, where $N = 1$ corresponds to a single-shot experiment [39]. As shown in Figure 6, it is evident that the QCRB undergoes a systematic decrease in conjunction with the augmentation of parameters s_1 and s_2 . This phenomenon is indicative of the realisation of an equivalent weak-value amplification effect through optimising the intrinsic properties of

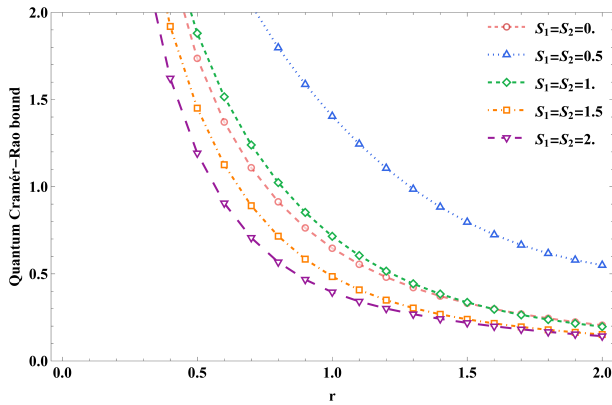


Figure 6. The quantum Cramér-Rao bound ($\delta\varphi$) for the state ($|\Phi\rangle$) is plotted as a function of r , with curves shown for different values of s . With fixed parameters $\mu = \varphi = \delta_1 = \delta_2 = \pi/2$ and $\theta_1 = \theta_2 = 4\pi/5$.

the quantum state. In this scenario, the augmentation of parameters s_1 and s_2 is analogous to the enhancement of the quantum resources of the ECSs, thus leading to an amplification of their sensitivity to phase alterations. This intrinsic quantum amplification mechanism has the effect of continuously compressing the precision limit ($\delta\varphi$) of phase estimation. This phenomenon is analogous to achieving enhanced sensitivity in parameter estimation through quantum resource optimisation, thereby demonstrating the formidable capability of quantum entanglement to surpass standard quantum limits.

VII. CONCLUSION

In this paper, we demonstrate that post-selected weak measurements can effectively enhance the non-classical properties of entangled coherent states. By tuning the interaction strength, the system undergoes a transition from an anti-squeezed to a highly squeezed state, as reflected in the joint Wigner function evolving from a symmetric distribution to a complex multi-branch interference pattern. A significant enhancement in entanglement is observed under the Hillery-Zubairy criterion, while quantum Fisher information analysis confirms improved phase estimation precision with increasing coupling strength. Our results establish a versatile weak-measurement framework for controlling continuous-variable entanglement, offering valuable insights for advances in quantum metrology [40, 41] and measurement-driven quantum state engineering.

VIII. ACKNOWLEDGMENTS

The computational work in this study, from mathematical derivations to visualizations, was carried out using version 14.3 of the Wolfram Language and the Wolfram quantum framework.

-
- [1] Y. Aharonov, D. Z. Albert, and L. Vaidman, *Phys. Rev. Lett.* **60**, 1351 (1988).
- [2] I. M. Duck, P. M. Stevenson, and E. C. G. Sudarshan, *Phys. Rev. D* **40**, 2112 (1989).
- [3] Y. Aharonov and L. Vaidman, *Phys. Rev. A* **41**, 11 (1990).
- [4] J. Yuanbek, Y.-F. Ren, and Y. Turek, *Phys. Rev. A* **111**, 063707 (2025).
- [5] B. de Lima Bernardo, S. Azevedo, and A. Rosas, *Opt. Commun.* **331**, 194 (2014).
- [6] J. Yuanbek, Y.-F. Ren, A. Abliz, and Y. Turek, *Phys. Rev. A* **110**, 052611 (2024).
- [7] Q. Hu, T. Yusufu, and Y. Turek, *Phys. Rev. A* **105**, 022608 (2022).
- [8] W. J. Xu, T. Yusufu, and Y. Turek, *Phys. Rev. A* **105**, 022210 (2022).
- [9] Y. Turek, J. Yuanbek, and A. Abliz, *Phys. Lett. A* **462**, 128663 (2023).
- [10] A. G. Kofman, S. Ashhab, and F. Nori, *Phys. Rep.* **520**, 43 (2012).
- [11] J. Dressel, M. Malik, F. M. Miatto, A. N. Jordan, and R. W. Boyd, *Rev. Mod. Phys.* **86**, 307 (2014).
- [12] B. E. Y. Svensson, *Quanta* **2**, 18 (2013).
- [13] D. Sokolovski, *Quanta* **2**, 50 (2013).
- [14] H. M. Wiseman and G. J. Milburn, *Quantum Measurement and Control* (Cambridge University Press, Cambridge, England, 2014).
- [15] J. Dressel and A. N. Jordan, *Phys. Rev. A* **85**, 012107 (2012).
- [16] J. Joo, W. J. Munro, and T. P. Spiller, *Phys. Rev. Lett.* **107**, 083601 (2011).
- [17] B. C. Sanders, *Phys. Rev. A* **45**, 6811 (1992).
- [18] H. Jeon, J. Kang, J. Kim, W. Choi, K. Kim, and T. Kim, *Sci. Rep.* **14**, 6847 (2024).
- [19] G. S. Agarwal and K. Tara, *Phys. Rev. A* **43**, 492 (1991).
- [20] A. Ourjoumtsev, R. Tualle-Brouiri, J. Laurat, and P. Grangier, *Science* **312**, 83 (2006).
- [21] M. Hillery and M. S. Zubairy, *Phys. Rev. Lett.* **96**, 050503 (2006).
- [22] G. C. Knee and E. M. Gauger, *Phys. Rev. X* **4**, 011032 (2014).
- [23] J. C. Howell, D. J. Starling, P. B. Dixon, P. K. Vudiyasetu, and A. N. Jordan, *Phys. Rev. A* **81**, 033813 (2010).
- [24] R. Horodecki, P. Horodecki, M. Horodecki, and K. Horodecki, *Rev. Mod. Phys.* **81**, 865 (2009).
- [25] V. Vedral, *Nat. Phys.* **10**, 256 (2014).
- [26] J. Tavares, *Rev. Ciência Elem* (2023).
- [27] T. Ono and H. F. Hofmann, *Phys. Rev. A* **81**, 033819 (2010).
- [28] A. Luis, *Phys. Rev. A* **64**, 054102 (2001).
- [29] C. Gerry and P. Knight, *Introductory Quantum Optics* (Cambridge University Press, Cambridge, England, 2004).
- [30] J. von Neumann, *Mathematical Foundations of Quantum Mechanics*, edited by N. A. Wheeler (Princeton University Press, Princeton, 2018).
- [31] G. Puentes, N. Hermosa, and J. P. Torres, *Phys. Rev. Lett.* **109**, 040401 (2012).
- [32] F. Hong-yi, *Phys. Rev. A* **41**, 1526 (1990).
- [33] M. Hillery, *Phys. Rev. A* **40**, 3147 (1989).

- [34] Nguyen Ba An and Vo Tinh, *Physics Letters A* **261**, 34 (1999).
- [35] Y. Kurochkin, A. S. Prasad, and A. I. Lvovsky, *Phys. Rev. Lett.* **112**, 070402 (2014).
- [36] G. Ren, W. hai Zhang, and Y. jun Xu, *PHYSICA A*, **520**, 106 (2019).
- [37] M. Hillery and M. S. Zubairy, *Phys. Rev. A* **74**, 032333 (2006).
- [38] F. Li, T. Li, and G. S. Agarwal, *Phys. Rev. Res.* **3**, 033095 (2021).
- [39] M. Zwierz, C. A. Pérez-Delgado, and P. Kok, *Phys. Rev. Lett.* **105**, 180402 (2010).
- [40] L. Xu, Z. Liu, A. Datta, G. C. Knee, J. S. Lundeen, Y.-q. Lu, and L. Zhang, *Phys. Rev. Lett.* **125**, 080501 (2020).
- [41] S.-Y. Yoo, Y. Kim, U.-S. Kim, C.-H. Lee, and Y.-H. Kim, *Quantum Sci. Technol* **10**, 025054 (2025).